Chem Soc Rev

This article was published as part of the

2008 Gold: Chemistry, Materials and Catalysis Issue

Please take a look at the full table of contents to access the other papers in this issue

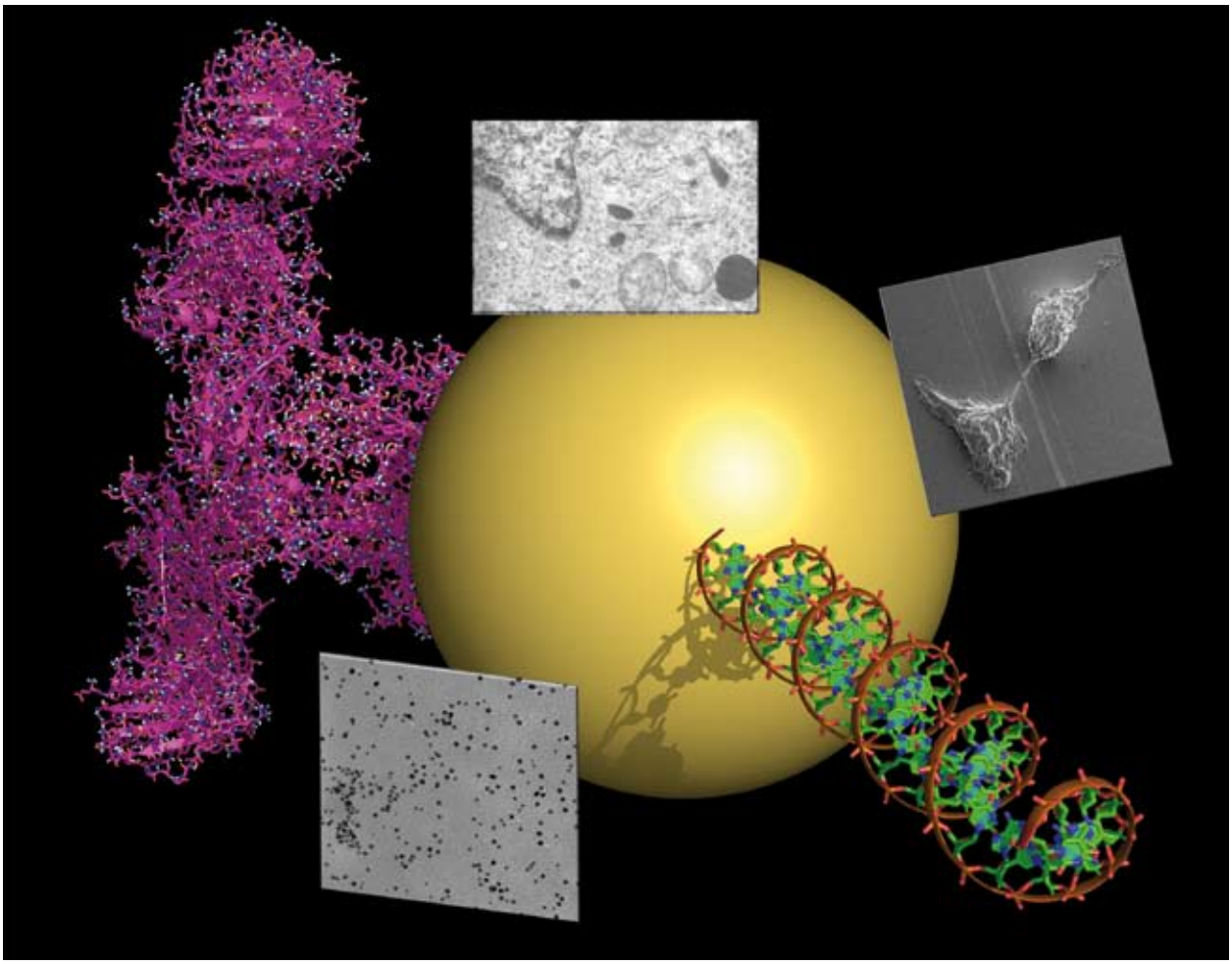

Gold nanoparticle superlattices†

B. L. V. Prasad,*[a] C. M. Sorensen[b] and Kenneth J. Klabunde[c]

Received 24th June 2008
First published as an Advance Article on the web 17th July 2008
DOI: 10.1039/b712175j

Ordered metal nanoparticle assemblies—superlattices—have captivated and stirred the imagination of scientists and engineers alike and promise great prospect for future technologies. This potential though will greatly be determined by the understanding and control that can be exerted on the assembling processes. This *tutorial review* presents a brief account of the factors that govern the formation of superlattices and then presents several examples of gold nanoparticle superlattices that are distinguished by the size of participating particles, chain length/functional group of the capping agent, the substrates on which they form *etc*.

1. Introduction

The need for miniaturization beyond the limitations of present lithographic techniques has been regarded as one main contributor to the current euphoria in nanoscience.[1] Fulfilment of this need requires making particles/systems in nanodimension and assembling them into required circuitry with appropriate connectors. The so-called ''bottom-up'' approaches have matured into a theme that could provide nanoparticles of different sizes, shapes and composition reproducibly, fulfilling the first requirement for future miniaturization needs.[2] However, the bottleneck for further developments lies in the assembly of these particles into precise hierarchical structures. Self-assembly or spontaneous assembly of nanoparticles is believed by many as the key for achieving such structures. This review provides a succinct description of the periodic structures that have been achieved using gold nanoparticles (Au NPs) and the factors central to such assemblies. While the laws governing such assemblies are common to many materials (especially of noble metal particles), keeping the theme of this issue in view, we restrict ourselves here to gold particle examples only. We also emphasize that as this is a tutorial review, not exhaustive but only representative references have been provided. While every care has been taken to represent all the detailed work available in literature we apologize for any omissions.

The first step in realizing the assemblies is obviously the synthesis of nanoparticles. There are now a plethora of metal nanoparticle syntheses reported. For the ease of formation and the size, shape and the environment-dependent beautiful optical variations they display, gold nanoparticles actually grab a major share of the reported literature. Readers are referred to many of the exhaustive reviews existing,[3] including some in the current issue for an update on the synthetic protocols. For the subject of this review we classify the synthetic procedures in two ways, aqueous/polar solvent based and non-polar solvent based. In doing so, the large section of literature concerning particles generated by evaporation, thin films grown on substrates—a subject to which the true ''superlattice'' term originally belonged—have not been taken into consideration. The ''superlattices'' (SLs) that we refer to are

[a] *Materials Chemistry Division, National Chemical Laboratory, Pune, 411 008, India. E-mail: pl.bhagavatula@ncl.res.in; Fax: +91 20 25902636; Tel: +91 20 25902013*
[b] *Department of Physics, Kansas State University, Manhattan, Kansas 66506, USA*
[c] *Department of Chemistry, Kansas State University, Manhattan, Kansas 66506, USA*
† Part of a thematic issue covering the topic of gold: chemistry, materials and catalysis.

B. L. V. Prasad

B. L. V. Prasad obtained his BSc in Vijayawada, and did his MSc and PhD in Chemistry (with T. P. Radhakrishnan) from University of Hyderabad, India. After postdoctoral stints at Tokyo Institute of Technology (with T. Enoki) and Kansas State University (with Chris Sorensen and Ken Klabunde) he joined National Chemical Laboratory, Pune, India as a scientist. He is currently working on nanoparticle synthesis, assembly and properties.

Christopher M. Sorensen (Chris) is University Distinguished Professor in the Departments of Physics and Chemistry (adjunct) and the Coffman Chair for University Distinguished Teaching Scholars at Kansas State University. He received a PhD in physics from the University of Colorado in 1976. His research concerns particulate systems and soft matter physics. In his spare time he enjoys sports, poetry and the night sky.

Kenneth J. Klabunde is University Distinguished Professor in the Department of Chemistry, Kansas State University. He received a PhD from University of Iowa in 1969. He has won several awards including Breakthrough Invention Award of Popular Mechanics Magazine, 2005; WESP Award for ''Making a Difference,'' in 2005. He is author/editor of several books and papers in the area of small particles and nanoscale materials.

the periodical nanoparticle/crystal arrays that are obtained from dispersions in solutions. These nanoparticles are prepared mainly by chemical reduction methods in either aqueous/polar or non-polar solvent media.

For the polar-medium based Au NP synthetic procedures, citrate and borohydride are probably the most popular reducing agents. When Au^{III} complexes at low concentrations (1×10^{-4}–5×10^{-4} M) are reduced with either borohydride or trisodium citrate quite stable as-prepared dispersions are obtained. On the other hand, the two-phase synthetic procedure pioneered by Brust–Schiffrin is one prevalent choice for obtaining non-polar nanoparticle dispersions.[4] This method involves the phase transfer of an Au^{III} complex from aqueous to organic solvent using a surfactant and a subsequent reduction of gold ions by sodium borohydride in the presence of a stabilizing/capping agent (ligand). Similar, ligand-stabilized nanoparticles can be obtained by the so-called reverse micelle or microemulsion method where the Au^{III} complex is dissolved directly in the organic medium containing the capping agent using a surfactant and few drops of aqueous solution of reductant is added subsequently.[5] While the aqueous medium based procedures generally lead to negatively charged particles, the two-phase procedures lead to what are referred to as ''monolayer protected clusters''. The experimental parameters in both these procedures can be tuned to obtain a fairly narrow size distribution of particles. This size distribution can further be narrowed by techniques such as size exclusion chromatography, size selective precipitation *etc*.[3b] An attractive alternative to these methods is digestive ripening where a polydisperse colloid is refluxed with a potential capping agent in a solvent such as toluene and is converted to a highly monodisperse system.[6] Once a reasonably monodisperse (generally a size variation $\leq$5% is considered good) system is available the SLs can be obtained either by assembly in solution or by drop casting on a substrate.

A further classification that we wish to make concerning the assemblies of nanoparticles of the two main subclasses indicated above is provided in Fig. 1. As noted we distinguish the assemblies mainly as those occurring in solution and those occurring on substrates. In both these instances the assembling process can be spontaneous or designed and each of these are specifically addressed in the respective sections assigned for them. However, before going into detail we present a brief account of the various competing forces that act on the nanoparticle dispersions and hence play a major role in determining the assembly processes.

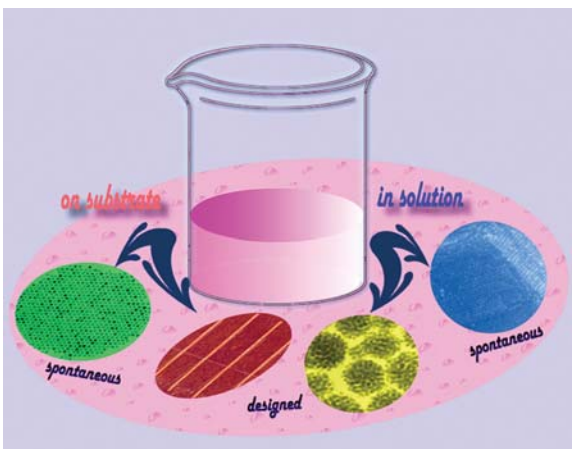

Fig. 1 A simple classification of nanoparticle assembly in solution and on substrates and the resulting structures that form. The images from left to right are taken and modified from ref. 6, 27, 36 and 50, respectively.

2. Nanoparticle dispersions: stability and the interactions that govern superlattice formation

Size distribution of the particles greatly influences the SL characteristics and indeed could decide whether SLs can form or not. Innumerable papers are present on this subject in literature especially regarding polymeric, SiO_2 colloidal particles ($\sim$200–500 nm sizes), as the crystallization of these particles is known to result in photonic band gap materials.[7] Detailed experimental and computational studies have lead to the conclusion that particles that occupy more than 49.4% of fluid volume start crystallizing and the non-uniformity of size (polydispersity) should not exceed a few percent. Best SLs are known to occur at $\sim$2–3% polydispersity while polydispersity in excess of 12% is known to suppress crystallization. Although kinetic factors were initially believed to be the reasons for such behaviour, recent studies based on comprehensive computational modelling, reveal that it is actually the free energy barrier to nucleation that dictates the course of crystallization. Classical nucleation theories suggest that the barrier to nucleation steadily decreases with increase in particle concentration. However, it has now been demonstrated that in the polydisperse samples even at high particle concentrations the free energy barrier passes through a minimum that prevents the formation of critical nuclei and overall an amorphous colloidal solid phase results.[8] Though such detailed theoretical/computational understanding of crystallization in Au NPs is unknown the same principles would be effective with little variations.

Monodisperse nanoparticle dispersions present either in polar/aqueous and non-polar organic solvent environments mainly experience two competing forces. In the aqueous phase these are the van der Waals (vdW) attractive forces between the metal cores and the repulsive forces between the charged surfaces. The dispersion stability emanating from such opposing forces and factors that affect this stability have been worked out in great detail by Derjaguin and Landau and by Verwey and Overbeek and is known as DLVO theory.[9] According to this theory the total potential energy as a function of the interparticle distance between two approaching charged particles is the sum of the vdW attraction between the cores and the electrostatic repulsion between the charged surfaces. In any colloidal system the surface charge on the particle with the counter ion concentration change in the surrounding environment results in the electric double layer (Fig. 2(A), inset). In this situation, the calculated total potential energy is known to have two minima when the size of the double layer is smaller than the particle radius. These regions are characterised by flocculation (aggregated material may be redispersed by agitation) and coagulation (irreversible aggregation) occurring at larger and smaller particle separations,

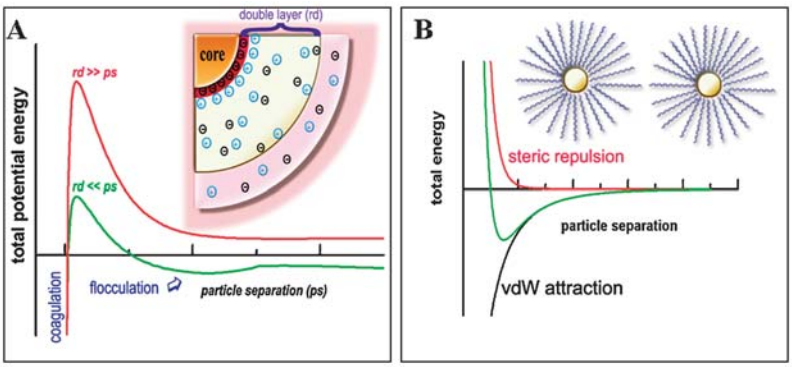

Fig. 2 The energy curves that describe nanoparticle stability in (A) polar solvents, where the nanoparticles are characterized by surface charges that cause repulsive interactions and (B) non-polar solvents, where particles are stabilized by ligand shells. In each case the attractive energy arises from the attractive forces between the metal cores and the subtle interplay between these and the repulsive interactions greatly influences the stability and ordered assembly formation (see text for more details).

respectively (Fig. 2(A)). When the double layer is larger than the particle radius only one minimum occurs and the particles coagulate irreversibly when the particle separation is small enough (Fig. 2(A)). In any case even small variations in electrolyte concentrations are known to change the characteristics of the electric double layer and hence affect the repulsive forces. Thus such aqueous suspensions are highly sensitive and can switch from a stabilized state to a destabilized state with only minor external changes.

As charged repulsive forces are so sensitive to the external environment, the stabilization imparted to the dispersion by thick ligand/polymeric shells (steric forces) is receiving much recent impetus. Initial developments in this area were focussed on obtaining non-polar organic solvent dispersions by using alkane thiols as capping agents on the nanoparticle surface.[4] The gamut of ligands have since been expanded to many other groups such as amines, silanes and phosphines *etc*.[10] In all these cases the total stability of the dispersion is again a combination of vdW attractive forces between the metal cores and the steric repulsive forces of the ligand shells. While Ohara *et al*. have treated the nanoparticles as "hard-spheres" and worked out a detailed expression for the vdW attractive forces between the gold cores through the solvent dodecane,[11] Korgel *et al*. by treating the nanoparticles as "soft-spheres" added a repulsive term emanating from the steric ligand shell.‡ This latter approach results in the expression[12] for total potential energy as a sum of metal core attractive forces (E_{vdW}) and the steric repulsive forces (E_{steric}) as given in eqn (1)–(3) (Fig. 2(B)).

$$E = E_{steric} + E_{vdW} \quad (1)$$

$$E_{vdW} = -\frac{A}{12}\left\{\frac{d^2}{s^2-d^2} + \frac{d^2}{s^2} + 2\ln\left(\frac{s^2-d^2}{s^2}\right)\right\} \quad (2)$$

$$E_{steric} = \frac{50dl^2}{(s-d)\pi\sigma_a^3} kT e^{-\pi(s-d)} \quad (3)$$

‡ A "hard sphere" is described as one that displays a sharp, infinitely strong repulsion upon touching another one, while a "soft sphere" exhibits gradually increasing repulsion as the separation is decreased.

In eqn (2) and (3), A is the Hamaker constant, d is the particle diameter, s the center to center interparticle separation, l the ligand chain length and σ_a, the area one thiol molecule occupies on the particle surface. Whereas the detailed calculations have all been done considering dispersions in non-polar organic solvents the same arguments can be extended to polar solvents where the dispersions are stabilized by thick polymeric/ligand shells. In either environment it is important that the ligand forms a complete layer and that one end of the ligand should be firmly anchored to the surface with the other end exposed to the "friendly" solvent environment. Otherwise, the van der Waals forces through the uncovered nanoparticle surface may lead to a net attractive force rendering the dispersions unstable. Addition of "non-friendly" solvents also disturbs and destabilizes the dispersion. We re-iterate that the forces considered above represent a simplified picture; other interactions could play a significant role in formation of SLs and significant progress is being made in understanding them. For example, Luedtke and Landman have shown that in crystals formed from particles the attractive interaction between ligand molecules (interdigitation or bundling) also plays a dominant role.[13]

A nanoparticle dispersion meeting the stabilization requirements mentioned above might remain unchanged for weeks/months to years under ideal conditions (particle and/or electrolyte concentration), where the steric/electrostatic repulsion compensates the vdW attractive forces. However, when a super-saturation type situation occurs the particles start self-assembling either in a solution or on a substrate. A critical nucleus formation ensues followed by an equilibrium process where particles in the surrounding solution of the nucleus attach to the nucleus. The nucleus will have a highly ordered particle arrangement while on the surface the ordering may not be perfect. These imperfectly ordered particles soon return to the solution while the perfectly ordered ones remain attached to the core contributing to its growth. After several such self correcting processes an equilibrium crystal forms that either precipitates or floats on the solution. These can then be taken for further investigations.

The SL formation can be probed *in situ* by techniques such as dynamic light scattering and small-angle X-ray scattering.

For the Au NPs case the optical absorbance methods present an easy alternative, as they are very sensitive to the interparticle distance.[14] When the particles do not have much interaction with the other particles in the dispersion a narrow peak in the optical absorbance spectra around 500 nm is seen for Au NPs. Although the nature of the peak and its position show dependence on the particle size and the solvent in which they are dispersed to a certain extent, a dramatic change in these two characteristics are seen once the particles start assembling. Thus a systematic optical absorbance study can provide much information about the assembling process especially in solution. Other techniques that are routinely used to probe the assemblies are electron microscopic techniques such as TEM (transmission electron microscopy) and SEM (scanning electron microscopy). While both these provide direct images of the SLs formed and thus invaluable information, TEM can also provide diffraction information that sometimes offers very good insight to the assembly processes. An excellent account by Zhang explains the different types of ordering possible in nanoparticle SLs and how electron microscopy can be utilized to study them.[15]

3. Superlattice structures—examples: in water and organic media

Despite the available understanding of different forces acting on the nanoparticles suspended in a solvent, the assemblies are usually obtained by evaporating a drop of the nanoparticle dispersion on a substrate. However, we present a few examples of SLs formed in solution first.

Indeed very few examples exist of SLs obtained (in solution) from Au nanoparticles stabilized by borohydride or citrate alone. Weitz and Oliveria[16] showed that addition of small amounts of pyridine to citrate-stabilized, highly monodisperse (14.5 nm) Au NPs actually results in fractal aggregates with a fractal dimension of 1.75. A fractal aggregate is an irreversible non-equilibrium structure.

Organic non-polar dispersions on the other hand are well studied. Whetten and co-workers have carried out careful fractional precipitation from solution and separated very narrow size fractions of different sized nanoparticles.[17] The near monodispersity in each case is so good that they show mass spectra prominently corresponding to one cluster size (same number of gold atoms in all the clusters) in the purified samples. Such samples when cast on a substrate show large areas of ultrathin SL structures (3–5 overlapping layers) with a great degree of orientational and translational order (Fig. 3(A)). Larger crystals (of several microns in size) were also grown by a slow precipitation method over a period of several days from a slowly stirred toluene–acetone solution of a highly purified fraction (Fig. 3(B)).

We have shown that toluene dispersions of nearly monodispersive Au NPs capped by octane-, decane- and dodecanethiol molecules obtained *via* the digestive ripening process, show purple precipitates at the bottom of the vial when left undisturbed.[6] TEM images obtained *via* drop casting of the solution obtained by simple shaking of these precipitates reveal the presence of 3-D SLs (Fig. 4(A)–(C)). Optical absorbance spectra support the contention that these SLs are formed in the solution and not on the TEM grid as the surface plasmon resonance peak is red shifted (Fig. 4(D)). Indeed, heating these dispersions to $\sim$80 °C does not reveal any red shift in the surface plasmon resonance (Fig. 4(E)) and drop casting a hot solution on a TEM grid reveals a reduced propensity to form a 3-D SL. Thus it can be safely concluded that the SLs shown in Fig. 4(A)–(C) were formed in solution. Subsequently it was shown that the types of SLs formed were very dependent on the nature of core nanoparticle that participates in the SLs.[18] For example, when single crystalline particles are participating they predominantly arrange in fcc lattices (Fig. 5(A); for the HRTEM images of individual particles, see Fig. 5(C) and (D)). Detailed structural analysis by HRTEM reveals a lattice parameter of 8.9–9.2 nm. On the other hand when the participating particles are characterized by defective structures predominantly hcp type assemblies with a lattice constant of 8 nm are seen (Fig. 5(B); for individual particles, see Fig. 5(E) and (F)). It can be safely argued that these are equilibrium structures as kinetic factors such as solvent evaporation rate, film drying, *etc*. have no influence on them. The reasons for the formation of fcc or hcp structures dependent on the particle type are not clear at the moment as calculations reveal that the energetic differences between hcp or fcc type ordering is very small.[19]

Abécassis *et al*. have recently probed Au nanoparticle SL formation in solution by *in situ* small-angle X-ray scattering when decanoic acid is used as capping agent.[20] They indicate

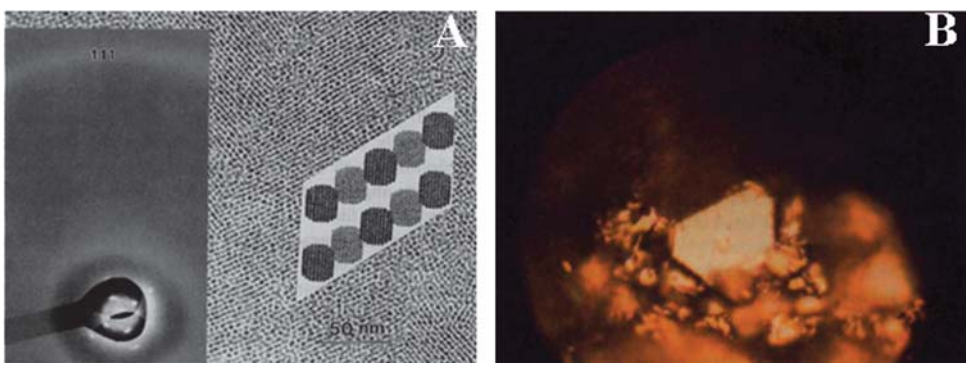

Fig. 3 (A) TEM images of highly ordered nanoparticle (particle size $\sim$2.4 nm) arrays reported by Whetten and co-workers. The corresponding electron diffraction and a suggested structural model are given in the inset. (B) Optical micrographs of micron sized crystals that were obtained by slow precipitation. Reprinted with permission from ref. 17. Copyright 1996, Wiley-VCH.

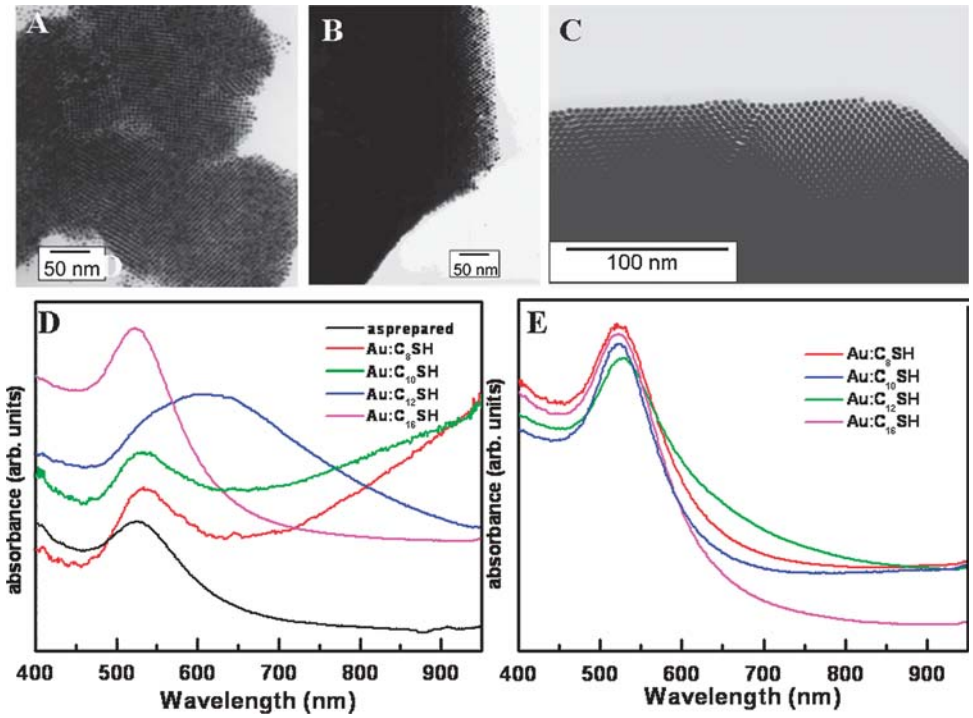

Fig. 4 Typical nanoparticle superlattice structures obtained from (A) octanethiol, (B) decanethiol and (C) dodecanethiol capped particles obtained *via* digestive ripening process. (D) A red shift in the peak at 525 nm or absorbance in the near-IR region of the optical absorbance spectra taken at room temperature asserts the formation of these assembled structures in solution and not on the TEM grid. (E) The crystals dissolve back in solution and show no red shift at 80 °C. Reprinted with permission from ref. 6 and 18. Copyright 2002 and 2003, American Chemical Society.

that in their case the assembly is only governed by attractive forces between the particles alone and no specific interaction between the capping agent exists. It is demonstrated that after the formation of particles is complete in 10 s, the SL formation is completed within 40–50 s; beyond this time the SLs coalesce and precipitate. The SL growth kinetics have been found to be slower than expected for a simple diffusion dependent process. Thus it is argued that the attractive forces between the particles play a major role in the assembly process.

In the following we discuss the influence of size, ligand effects (possessing different head groups and chain length) on the SL formation. In doing so, as the information available on the assembly processes in solution alone is rather limited, we also considered SLs formed on substrates. Here additional interactions such as solvent–substrate and particle–substrate interactions may influence the SL formation. However, these are expected only to interfere with the whole assembly process to a very limited extent, especially when substrates such as

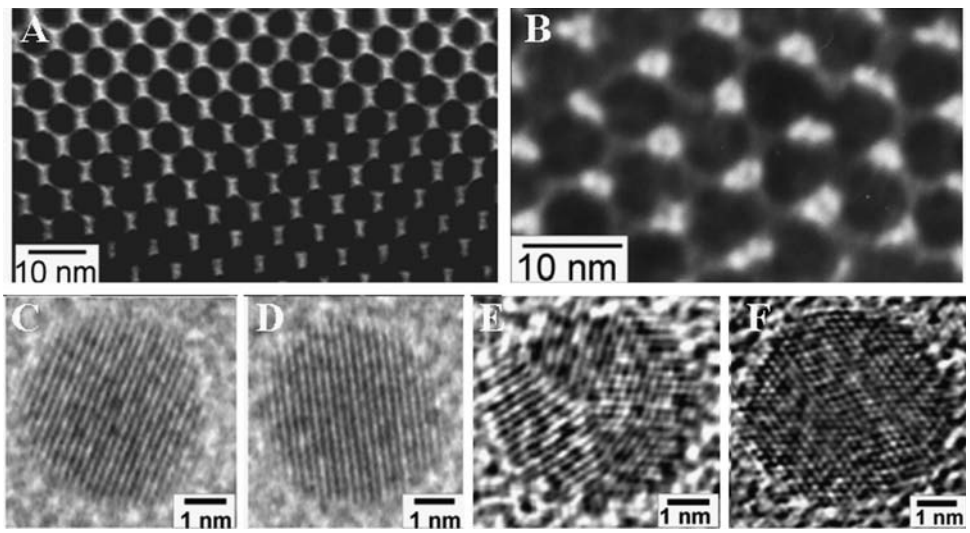

Fig. 5 (A) fcc and (B) hcp type assemblies formed from particles that are characterized as single crystalline (C–D) or defective (E–F) particles, respectively. Reprinted with permission from ref. 18. Copyright 2003, American Chemical Society.

TEM grids are used. Other substrates (patterned, functionalized *etc.*), where the assembly processes are mainly dependent on particle–(modified) substrate interactions, are discussed later.

4. Factors governing superlattice formation

4.1 Size

Systematic studies of the size-dependent variation in the formation of Au nanoparticle SLs are rather few though such detailed studies on thiol-capped Pd nanoparticles have been reported.[21] For Pd it has been clearly shown that the phase diagram of the SLs depends on the d/l ratio (where d is the particle diameter and l the length of capping agent).

A comprehensive report on the formation of SLs from particles of different sizes but capped by the same ligand was provided by Brown and Hutchison.[22] They have shown that pentadecylamine capped Au nanoparticles of different sizes varying between 1.8–8 nm demonstrate different types of SLs. They have also examined this SL formation at several stages namely, (i) SLs formed from dilute solutions cast on TEM grids, (ii) SLs formed as precipitates and (iii) small SLs as they are forming. From a detailed and careful analysis of electron diffraction they have demonstrated that small 1.8 nm particles self assemble into structures that possess predominantly translational ordering while bigger $\sim$8 nm nanoparticles (especially observed from precipitates or concentrated solutions) display both translational and rotational ordering (Fig. 6(A) and 5(B)). Obviously the latter must have been the result of an equilibrium process of crystallization.

In the previously mentioned study of Abécassis *et al*. also it is shown that the SL formation is dependent on particle size and that particle sizes larger than 4 nm only tended to form SLs.[20] They argued that for the capping agent they employed, at smaller particle sizes the thermal energy is sufficiently higher than the vdW attractive forces between the particles dispersing the particles away and hence a self assembly process is not possible. They also indicated that for particles that are too large the attractive forces will be too strong for the clusters to organize into crystalline equilibrium structures and in this case amorphous (fractal) structures form.

Kiely *et al*. observed the interesting formation of an ordered mixed array of particles with two different sizes (bimodal distribution).[23] More specifically when particles of 4.5 $\pm$ 0.8 and 7.8 $\pm$ 0.9 nm diameter are intricately mixed and drop casted on a TEM grid, spontaneous assembly similar to a AB_2 lattice type that is isostructural, for instance, with the alloy AlB_2 was observed. This clearly established a resemblance between atomic scale systems such as intermetallic alloys and the nanoparticles.

4.2 Ligand effects

Again a systematic study of same size nanoparticles that are capped by different monofunctional ligands is not available. Nevertheless, nanoparticles of similar size but capped by different monofunctional ligands are not expected to behave very differently in terms of their assemblies. This is because in any case, the head group would be anchored to the nanoparticle surface firmly and the hydrophobic alkane chain ($-CH_3$ group), similar in every aspect, is exposed to the exterior.

Even then, we have shown that amine-capped and alkane thiol-capped Au nanoparticles may show slight differences in their assemblies.[10] In this example the digestive ripening process was used where a polydisperse colloid in toluene is refluxed with dodecylamine or dodecanethiol to obtain $\sim$9 or 4.5 nm sized particles, respectively. Then, following the principles of the total potential energy laid out above (vdW attractive forces + the steric repulsive forces)[12] one would expect the larger sized particles (dodecylamine capped) to have more attractive energy towards one another and hence bigger/better propensity to form SLs. However, both the optical spectra and the TEM results indicate that smaller sized dodecanethiol capped particles form better 3-D SLs as compared to the amine capped ones. It should be noted that as both these molecules contain 12 carbon atoms the ligand shell on the surface is expected to be of the same thickness. It could be argued that the amine capped particles, as they posses stronger attractive forces owing to larger metal core sizes, crash out as small SLs thus preventing the formation of an equilibrium structure. This argument however is negated by evidence from optical absorbance studies that show no red shift that would indicate SL formation in solution. It is also shown that while the ligand shells from neighbouring Au particles in the thiol case participate in full interdigitation, ligands with amine head group do not do so (Fig. 7(A) and (B)). This has been partially attributed to the weaker binding

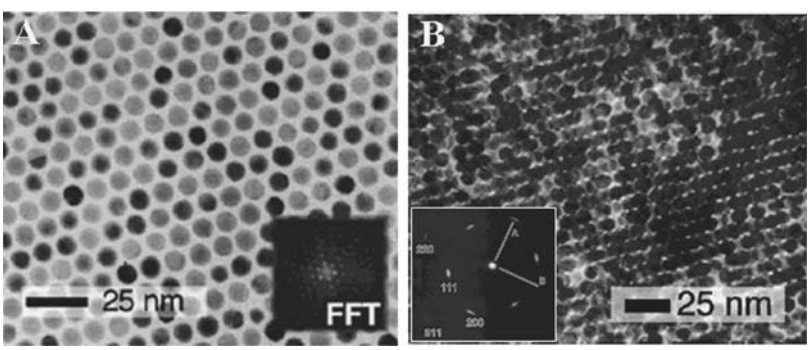

Fig. 6 TEM images of pentadecylamine capped Au NP assemblies obtained under different conditions. While the image and the fast-Fourier transform in (A) indicate long-range translational order, the arrangement and the diffraction in (B) clearly show long-range translational and orientational order. Reprinted with permission from ref. 22. Copyright 2001, American Chemical Society.

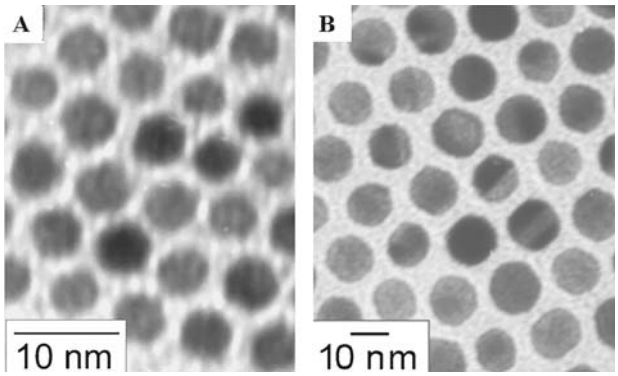

Fig. 7 Magnified TEM images of (A) dodecanethiol- and (B) dodecylamine-capped nanoparticle assemblies. Note the difference in interparticle distance in each case though both are capped by molecules with 12 carbon atom chain lengths. Reprinted with permission from ref. 10. Copyright 2003, American Chemical Society.

of the amine head group to the NP surface. Such weak binding may result in a higher disorder in the alkane chain and hence preventing interdigitation.[10]

4.3 Chain length variation of the ligand

Among the literature available this subject has been studied in a detailed manner. Fink *et al*. have prepared particles capped by quaternary ammonium bromides of varying chain lengths (C_6 to C_{18}).[24] It was shown that these particles self assemble into 2-D and 3-D assemblies on substrates and that the interparticle separation gradually increases as the chain length is increased. An interesting formation of multilayers where the particles occupy 2-fold saddle sites instead of 3-fold hollow sites is observed and attributed to the interplay between the electrostatic repulsion and vdW attractive forces. Martin *et al*. were the first to study the systematic variation of the thiol chain length on the nanoparticle surface with respect to the particle size variation and interparticle separation.[25] They had also studied the substrate effects, the presence and absence of surfactant, aging of the colloid and addition of a high boiling solvent to the nanoparticle dispersion. In the thiol chain length variation experiment, it was observed that as thiol chain length increases, the gap between the particles increases by 1.2 Å gap/carbon atom. The particles are always separated by one chain length distance as compared to the expected two chain length distance between nanoparticle surfaces indicating a good degree of interdigitation between the chains of adjacent particles. They have also shown that particles capped with dodecanethiol form nice 3-D crystals on Teflon substrates and the crystal growth improved on adding higher boiling alkanes such as dodecane or retaining the surfactant in which they are prepared. These may slow down droplet evaporation on the substrate and hence facilitate equilibrium crystal formation.

We have reported a detailed study on the effect of alkanethiol chain length on the nature and propensity to form SLs subsequently.[6] In this work the alkanethiol chain length was varied from octane to hexadecanethiol (C_8, C_{10}, C_{12} and C_{16} chain lengths were considered). Polydisperse Au NPs prepared *via* an inverse micelle method were subjected to digestive ripening with above listed thiols. The resulting monodisperse particles when left undisturbed formed precipitates at the bottom. Interestingly in Au–C_8SH case all the nanoparticle dispersions precipitated at the bottom leaving a colorless supernatant. For Au–C_{10}SH and Au–C_{12}SH some nanoparticles remained suspended in the solution while a majority of them precipitated. For Au–C_{16}SH no precipitate formed at the bottom and all the nanoparticles remained suspended in solution. Optical absorbance spectra of vigorously shaken solutions corroborate the visual inspection details described above (Fig. 4(D)). For Au–C_8SH and Au–C_{10}SH apart from the surface plasmon resonance peak a second absorbance maximum running into the near-IR region is observed. Such maxima are attributed to interacting nanoparticles in solution. The extent of red shift is clearly an indication of greater extent of aggregation (greater red shift = smaller interparticle separation and larger aggregates). These aggregates when imaged with a TEM turned out to be ordered assemblies and results can be summarized as follows. For Au–C_8SH case only 3-D aggregates are seen. Au–C_{10}SH and Au–C_{12}SH also reveal 3-D aggregates though small areas of 2-D hcp arrangements could as well be seen while Au–C_{16}SH only displays 2-D monolayer arrangements. The vdW attractive forces determined using the equation provided by Ohara *et al*.[11] provides some quantitative insight to these observations. The values were determined to be $5k_BT$, $2.2k_BT$, $2k_BT$ and $0.6k_BT$ for the Au–C_8SH, Au–C_{10}SH, Au–C_{12}SH and Au–C_{16}SH nanoparticle dispersions, respectively. This indicates that for Au–C_8SH the attractive forces between the particles are very large leading to 3-D SL formation and precipitation. For Au–C_{10}SH and Au–C_{12}SH the attractive forces are not very large and the thermal energy would try to keep the particles apart. For the same reason the nuclei in these cases may undergo lot of self correction through formation and dissolution thus leading ultimately to good equilibrium structure formation. It should be noted that most of the best SL structures reported in literature have dodecanethiol as the capping agent. For Au–C_{16}SH, nanoparticles are apparently prevented from interacting by the thermal energies. However, on the substrate when the solvent evaporates they form large 2-D monolayers. As has been pointed out earlier all these systems show no precipitates and thus no red shift (Fig. 4(E)) in the surface plasmon resonance when heated to $\sim$80 °C in toluene, indicating that the superlattice crystals formed dissolve back in the solution at these temperatures. This is very similar to molecular crystallization processes.

5. Assemblies through bifunctional molecules

5.1 Dithiols

Almost immediately after reporting the synthesis of alkanethiol capped nanoparticles in organic solvents Brust *et al*. reported their assemblies by use of α,ω-dithiols.[26] The assembly process is induced because each thiol molecule can attach to two nanoparticles. However, as can be easily expected it is very difficult get a complete control over this assembly process as it is known to occur in a random fashion. Brust *et al*.,

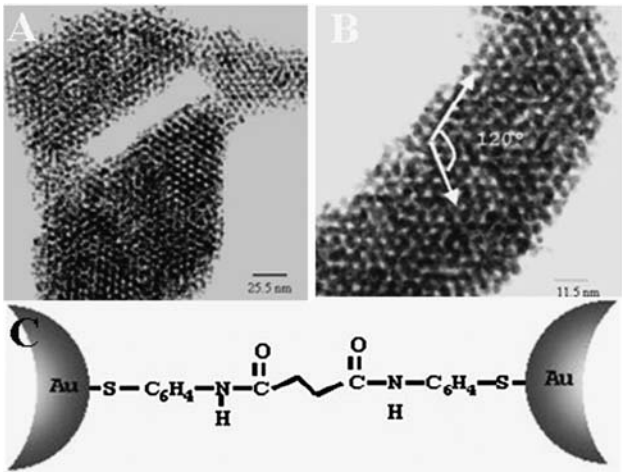

Fig. 8 (A–B) Nanoparticle assemblies mediated by post-synthetic linking of capping molecules. (C) The particles are initially capped by mercaptoaniline and the exposed amine groups on two nanoparticles are subsequently linked by succinyl chloride. Reprinted with permission from ref. 28. Copyright 2002, Wiley-VCH.

however, were able to introduce some ordering into these assemblies by controlling the amount of dithiols added.[26] More recently, they have been able to manipulate these aggregates in a more controllable way by adding measured amounts of ethanol.[27] In any case, the resulting aggregates are always spherical and obtaining a 3-D ordered crystalline array seems to be difficult with this procedure. Mayer *et al*. were able to bring a great degree of order (Fig. 8) to this process by modifying the nanoparticle surface with mercaptoaniline and linking the exposed amine groups with succinyl chloride.[28] Modification of this strategy (linking two nanoparticles with a dithiol) has led to many interesting prospects. For example, some of us have reported photoresponsive nanoparticle networks (Fig. 9) by designing dithiols having azobenzene groups.[29] As the azobenzene undergoes light induced *cis–trans* conformational changes the nanoparticle networks linked by these molecules become denser (Fig. 9, panel IIC) or expanded (Fig. 9, panel IID). Such photo-induced changes can be repeated a few times. Similarly cleavable Au NP networks have also been reported that are linked again by dithiols but with cleavable carboxylate ester groups.[30]

Although the assembling process achieved by the dithiol linkers are generally random, especially in solution, some attractive assembling strategies have been reported by adapting layer-by-layer assembly processes.[31]

5.2 Hydrogen bonding

Some of the best examples of SLs have been reported under this category. Rotello and co-workers have been using the molecular assembly methods where the assembly of the nanoparticles is driven by the specific interaction between complimentary recognition units. They call this the ''brick and mortar'' strategy where the nanoparticle surface capping units and the recognition units that bind to them specifically bring the particles together.[32] Other celebrated examples in this repertoire include the DNA mediated assemblies investigated in great detail by Mirkin and co-workers.[33] Further details on these studies can be obtained in many reviews, some of them in this issue. Klabunde and co-workers have examined various water-soluble ligand-stabilized nanoparticles synthesized *via* an evaporation based route.[34] Some of them were seen to result in significantly narrow size distributed particle systems leading to formation of 2-D or 3-D assemblies on TEM grids that could be mediated by hydrogen bonding.

Highly ordered nanoparticle assembly systems that have been investigated thoroughly by Kimura's group (Fig. 10(A) and (B)) are Au NPs capped by mercaptosuccinic acid.[35] The successful organization of these nanoparticles into beautiful 3-D structures in solution may be attributed to the addition of acid (pH $\leq$2) to the nanoparticle dispersions. This is expected to keep the exterior functional groups in the carboxylic acid form rather than the carboxylate form. They argue that this

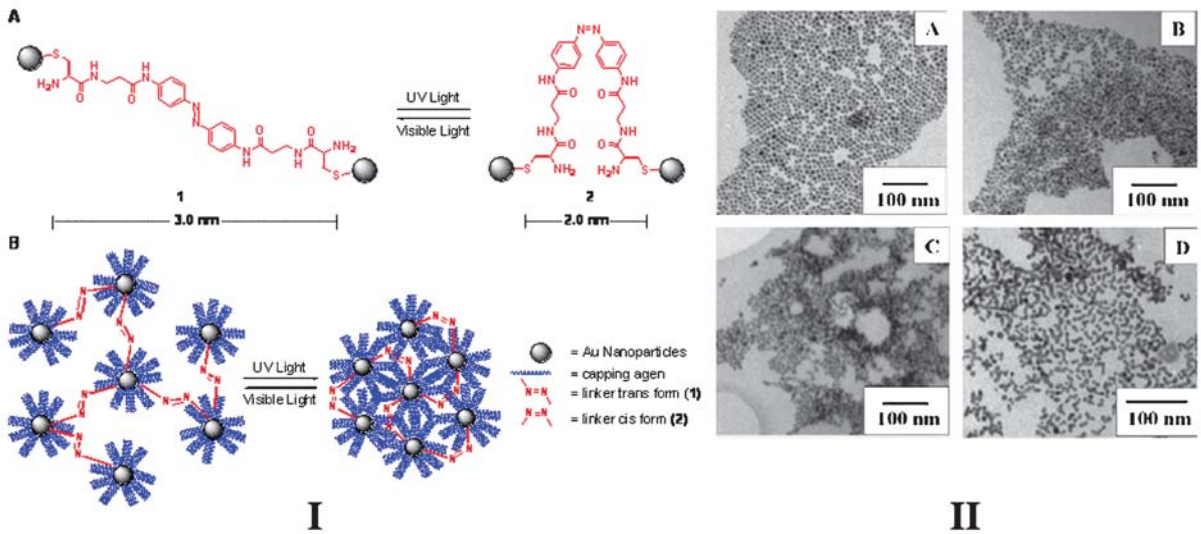

Fig. 9 (I) Schematic illustration of photo-responsive nanoparticle networks. The particle networks are brought together or expanded by the conformational changes in the linker molecule between *cis* (**1**) and *trans* (**2**) forms. (II) The changes occurring in TEM images concur with the photo-responsive hypothesis. See text for details. Reprinted with permission from ref. 29. Copyright 2005, American Chemical Society.

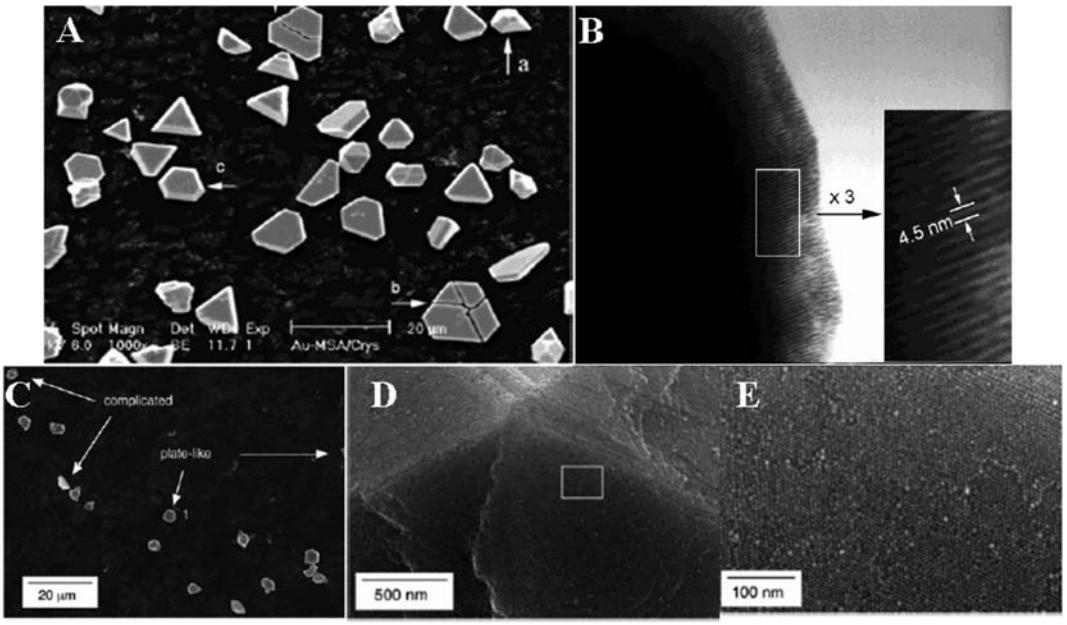

Fig. 10 (A) FE-SEM and (B) HRTEM images of superlattice structures of mercaptosuccinic acid capped nanoparticles. Reprinted with permission from ref. 35. Copyright 2003, American Chemical Society. (C–E) FE-SEM images of *n*-acetylglutathione capped nanoparticle crystals. Reprinted with permission from ref. 36. Copyright 2006, American Chemical Society.

would make the assembly process slower thus enabling the equilibrium structures to form. The –COOH groups present on two adjacent nanoparticles have been shown to be involved in hydrogen bonding. The particles assemble in an hcp structure with a unit cell parameter of 5.1–5.2 nm. Very recently the same group has reported striking SLs (Fig. 10(C)–(E)) grown from *n*-acetylglutathione capped nanoparticles again by allowing the crystallization process to take place under acidic condition.[36] This time the particles self assembled into an fcc structure with a lattice parameter of 11.1 nm. An interesting feature here is the observation of five-fold symmetry in these SLs stemming from the multiple twinning.

6. Assemblies at the air–water interface

The air–water interface has been one popular choice for the preparation and assembly of nanomaterials. The air–water interface allows the assembly of hydrophobic nanoparticles as they can form monolayers at the interface. These can be subjected to different barrier pressures leading to different types of assemblies. Hydrophilic nanoparticles can also be assembled at the air–water interface by spreading oppositely charged molecular/polyelectrolyte monolayers at the interface. The nanoparticles present in the water sub-phase electrostatically interact with the charged molecules at the interface thus leading to the assembly. Fendler *et al.* have pioneered the utility of the air–water interface for the assembly of various structures.[37] Wei and co-workers have utilized the air–water interface to assemble resorcinarene-tetrathiol encapsulated Au NPs of varying sizes that formed nice hcp ordered arrays.[38] Kimura and co-workers assembled their mercaptosuccinic acid capped Au NPs at the air–water interface using bifunctional external hydrogen bonding mediators and were also able to control the interparticle spacing.[39] Sastry and co-workers used the air–water interface extensively to assemble, prepare and modify the nanoparticle surface. Features of their work include assembly of hydrophilic nanoparticles through their electrostatic complexation with monolayers of fatty acids or fatty amines, synthesis of nanoparticles with multifunctional monolayer forming molecules, heterocolloidal multiparticle films *etc*. They have also used thermally evaporated lipid films for the assembly of nanoparticles that behave very similarly to the Langmuir–Blodgett films lifted onto a substrate.[40]

7. Assemblies at the liquid–liquid interface

Liquid–liquid interfaces also started attracting the attention of researchers for the preparation and assembly of nanoparticles. Sastry and co-workers have shown that aqueous nanoparticles can be assembled into films at the liquid–liquid interface using benzene or anthracene.[41] Later they extended the liquid–liquid interface work where molecules such as hexadecylaniline having dual capability (that of electrostatically binding to the nanoparticle surface and reducing ability) were used to synthesize nanoparticles or assemble them at the interface.[42] Rao and co-workers exemplified the great potential and the simplicity of this technique through the synthesis, assembly and properties of various nanoparticles and particle assemblies including Au at the liquid–liquid interface.[43] In a typical reaction the gold precursor in toluene was allowed to react with tetrakis(hydroxymethyl)phosphonium chloride in water. The water and toluene solutions are present in the same beaker and the reaction occurs at the interface leading to the formation of free standing metal films.[44] By varying the reaction temperature a great degree of control in the nature of nanoparticle films could be obtained (Fig. 11). Generally films formed at lower temperature revealed spherical particles of narrow size

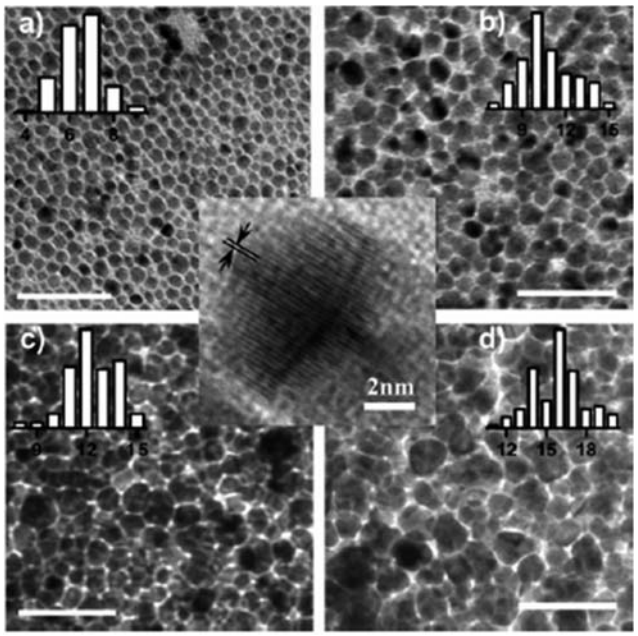

Fig. 11 Au nanoparticles prepared at the liquid–liquid interface at (a) 30, (b) 45, (c) 60 and (d) 75 °C. Inset shows a high resolution image of one particle. Reprinted with permission from ref. 44. Copyright 2005, American Chemical Society.

distribution while the films formed at higher temperatures showed larger particles with broad size distribution and narrow interparticle distance. The measured resistance of the films obtained at lower temperatures is in the mΩ range while those formed at higher temperature is in kΩ range. Similar trends were also observed when the films are treated with alkanethiols of varying chain length; here larger chain length thiols leading to greater particle separation and shorter ones with smaller particle separations.[44] Thus the liquid–liquid interface offers great possibilities for the synthesis and assembly of nanoparticles with different properties.

8. Assemblies on substrates

8.1 Substrate effects

TEM grids are by far the most utilized substrates in so far as the demonstration of assemblies is concerned. A great degree of variation in the assembly process on TEM grids is reported and bringing a systematic order to the available literature on this subject is indeed an uphill task.

Gelbart and co-workers have published a series of papers backed up by systematic computer simulations explaining the formation of annular rings when a drop of dilute nanoparticle dispersion in nonpolar organic solvents evaporates on a TEM grid.[45] Same type of assemblies can be obtained on suitable substrates that are fairly hydrophobic such as organically modified Si, HOPG or Teflon where the hydrophobic solvent wets the surface uniformly. Lin *et al*. obtained beautiful long range orders of ~4.5 nm Au NPs passivated by dodecanethiol on thinned SiN substrates (Fig. 12) that can be directly imaged by an electron microscope.[46] They have shown that a little

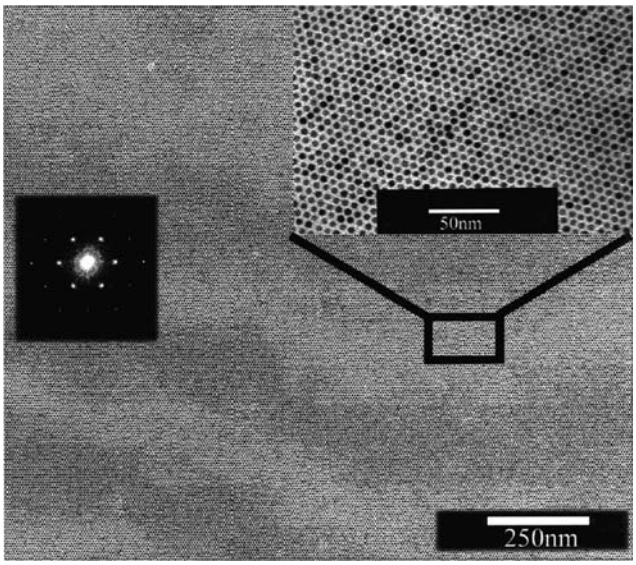

Fig. 12 A long-range two-dimensional ordered array of dodecanethiol-capped gold nanoparticles on SiN substrate. Reprinted with permission from ref. 46. Copyright 2001, American Chemical Society.

additional dodecanethiol helps in slowing down the evaporation process thus aiding in the long-range assembly formation. Non-polar solvents do not wet hydrophilic substrates such as mica or glass thus affecting the SL quality. Using grease to contain the droplet or modifying the glass surface with a carbon film similar to that done for a TEM grid seems to improve the SL quality dramatically.[24] Korgel and Fitzmaurice, by incorporating the substrate–particle and substrate–solvent interactions worked out conditions for solvent drop thickness when a dispersion drop is cast on a substrate.[47] According to them this depends on S; the spreading coefficient given by:

$$S = \gamma_{sub,sol} - (\gamma_{NP,sub} + \gamma_{NP,NP})$$

where $\gamma_{sub,sol}$, $\gamma_{NP,sub}$ and $\gamma_{NP,NP}$ are the surface tensions of substrate–solvent, nanoparticle–substrate and nanoparticle–nanoparticle, respectively. It was found that varying the polarity of the solvent greatly affects the film thickness and thus the propensity to form monolayers or multilayers when nanoparticle dispersions are drop cast on TEM grids. It was shown that increasing the amount of ethanol added to the chloroform supported the formation of smaller films with greater thickness thus supporting the 3-D monolayer formation. On the other hand dispersions of same concentrations cast from chloroform solution alone lead to only monolayer formation.

8.2 Chemical functionality of the substrate-SAMs and their modifications

More systematic variation to the chemical functionality of the substrate can be imparted through the formation of self assembled monolayers (SAMs) on the surface. In fact many of the dithiol mediated assemblies (especially growing 3-D films) utilize this process.[30] The SAMs could be made of simple monofunctional alkanethiol molecules with an exposed hydrophobic moiety that can be used to assemble hydrophobic

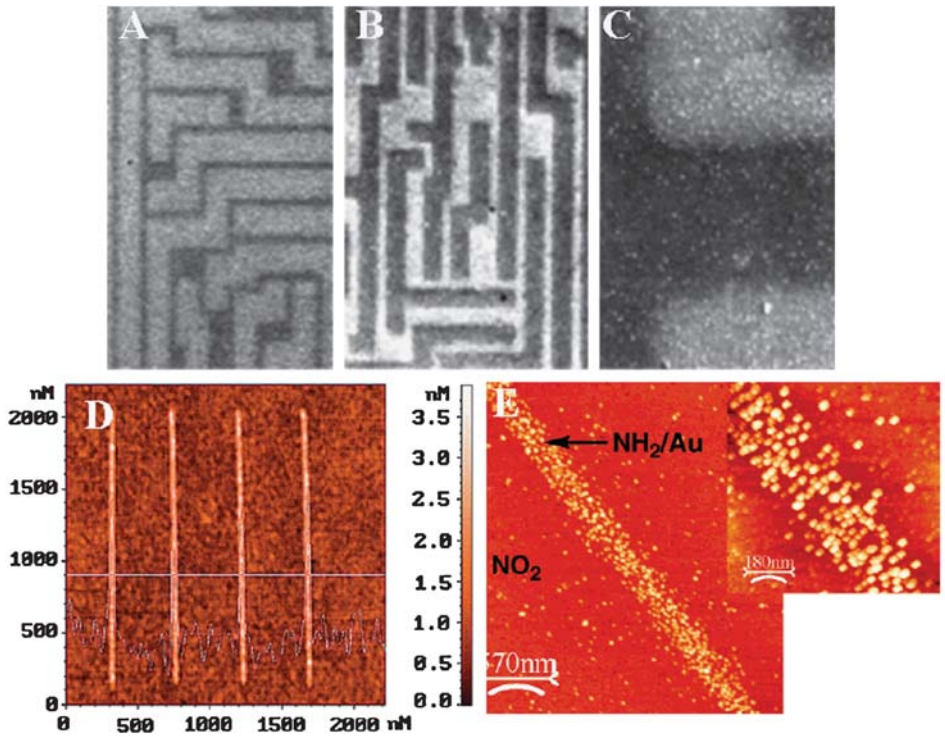

Fig. 13 Self assembled monolayer based strategies for patterning arrays of gold nanoparticles on substrates. (A–C) the substrates are first patterned by photocleavable organic molecules that expose $-NH_2$ upon light exposure. These are then dipped in amine-capped nanoparticles. Reprinted with permission from ref. 49*a*. Copyright 1997, Wiley-VCH. (D) The substrates are modified/patterned with AFM tip so that –SH groups are exposed wherever a pattern with AFM tip is written. Subsequent exposure of the substrate to Au_{55} clusters capped by phosphine ligands completes the assembly process. Reprinted with permission from ref. 49*b*. Copyright 2002, American Chemical Society. (E) The substrates are modified to expose $-NO_2$ groups that are reduced to $-NH_2$ groups in a pattern on electron beam irradiation. A dipping of the substrate in acidic citrate stabilized nanoparticle dispersion concludes the assembly process. Reprinted with permission from ref. 49c. Copyright 2004, American Chemical Society.

Au NPs.[48] On the other hand SAMs of bifunctional molecules have been very intelligently used (Fig. 13) to generate highly ordered linear assemblies.[49] The typical methods describing such assembly processes are given below. In all these processes the first step is to covalently modify the required surface with a bifunctional silane molecule. Schmid and co-workers used an AFM tip to convert the terminal $-CH_3$ groups of octadeylsilane to –COOH groups.[49*b*] Further reaction of these –COOH groups with appropriate reagents lead to the generation of surface thiol groups wherever the –COOH pattern was written earlier (Fig. 13(D)). Finally dipping these thiol patterned substrates simply into Au_{55} clusters decorated the thiol pattern written with Au particles. Truly single particle lines of Au_{55} particles could be developed using this simple process. Mendes *et al.* used 3-(4-nitrophenoxy)propyltrimethoxysilane as a modifying agent so that a substrate with exposed nitro groups is realized.[49*c*] These nitro groups were then reduced to amine groups by e-beam lithography so that the e-beam exposed areas specifically converted to $-NH_2$ groups (Fig. 13(E)). Then at acidic pH conditions these patterned substrates are dipped into dispersions of negatively charged Au NPs. As the negative charged Au NPs only interact with $-NH_3^+$ groups on the surface (the written pattern) the pattern is truly replicated by the nanoparticles.

9. Miscellaneous techniques

There are several other techniques/examples that could not be covered because of space limitations. Most notable among them are the DNA mediated assemblies,[50] assemblies/patterns obtained by Dip-pen lithography *etc.*[51] Schmid and co-workers[52] and Yang's group[53] have reported a "stick and slip" type model for fabricating one-dimensional assemblies on suitably modified surfaces from particles spread at an air–water interface. This was simply accomplished by dipping and withdrawing suitable substrates from a water surface at programmed speeds. Teranishi and co-workers reported several procedures for 2-D assemblies using novel ligand designs that can have groups participating in π–π interactions[54] or acid–base reactions.[55] Some of us have recently illustrated an *in situ* formed template mediated linear assembly of hexadecanethiol coated Au NPs.[56]

10. Applications and conclusions

The most celebrated applications are from DNA-mediated Au NP assemblies.[32] Many reports also exist where these assemblies have been used as sensors.[57] However, many of them are from random assemblies and may actually do not show

ordered assemblies that can be truly called SLs. Properties of ordered assemblies are presently being probed in detail and many examples exist where the conductivities of the assemblies crucially depend on the interparticle separation. Other properties and applications of assemblies are being vigorously studied.[58] Gold superlattices will prove effective as capacitors, optical sensors, and pressure sensors. Understanding and reproducibly making assemblies in requisite fashion is expected to enable us to gain access to the fascinating world of ''metamaterials''.[59] They also are of interest as ''crystals of superatoms''; it would be interesting to see how they compare in structure to crystals of atoms. Ultimately, superlattices are controlled by the ligands. Therefore, ligand modifications will lead to hundreds of new structures. Finally assembling nanoparticles into desired, precise patterns with a reliability as close to that of the current lithography techniques may be the real basis for future technological developments as mentioned in the Introduction. Much more development is required before a high throughput process for the assembly of nanoparticles into pre-determined patterns can be really accomplished, and the investigations presented in the current review definitely provide ample hope that it is not an impossible task.

Acknowledgements

We thank all our collaborators who contributed to our work cited here. B. L. V. P. thanks DST for funding through a grant to NCL for Unit on Nanoscience and Nanotechnology. B. L. V. P. also thanks Dr C. V. Ramana for help in preparing the figures. The support of NASA and the NSF-NIRT grants are acknowledged with gratitude.

References

1 G. Schmid and U. Simon, *Chem. Commun*., 2005, 697–710.
2 J. Park, J. Joo, S. G. Kwon, Y. Jang and T. Hyeon, *Angew. Chem., Int. Ed*., 2007, **46**, 4630–4660.
3 (*a*) M.-C. Daniel and D. Astruc, *Chem. Rev*., 2004, **104**, 293–346; (*b*) J. A. Dahl, B. L. S. Maddux and J. E. Hutchison, *Chem. Rev*., 2007, **107**, 2228–2269.
4 M. Brust, M. Walker, D. Bethell, D. J. Schiffrin and R. Whyman, *J. Chem. Soc., Chem. Commun*., 1994, 801–802.
5 M. P. Pileni, *J. Phys. Chem. C*, 2007, **111**, 9019–9038.
6 B. L. V. Prasad, S. L. Stoeva, C. M. Sorensen and K. J. Klabunde, *Langmuir*, 2002, **18**, 7515–7520.
7 P. N. Pusey and W. van Megen, *Nature*, 1986, **320**, 340–342.
8 S. Auer and D. Frenkel, *Nature*, 2001, **413**, 711–713.
9 While DLVO theory is classic text book material now with any standard physical chemistry text book providing the theory, a good account of its application to Au NPs can be found in T. Laaksonen, P. Ahonen, C. Johans and K. Kontturi, *ChemPhysChem*, 2006, **7**, 2143–2149.
10 B. L. V. Prasad, S. I. Stoeva, C. M. Sorensen and K. J. Klabunde, *Chem. Mater*., 2003, **15**, 935–942.
11 P. C. Ohara, D. V. Leff, J. R. Heath and W. M. Gelbart, *Phys. Rev. Lett*., 1995, **75**, 3466–3470.
12 B. A. Korgel, S. Fullam, S. Connolly and D. Fitzmaurice, *J. Phys. Chem. B*, 1998, **102**, 8379–8388.
13 W. D. Luedtke and U. Landman, *J. Phys. Chem*., 1996, **100**, 13323–13329.
14 (*a*) P. Mulvaney, *Langmuir*, 1996, **12**, 788–800; (*b*) K. L. Kelly, E. Coronado, L. Li. Zhao and G. C. Schatz, *J. Phys. Chem. B*, 2003, **107**, 668–677.
15 Z. L. Wang, *Adv. Mater*., 1998, **10**, 13–30.
16 D. A. Weitz and M. Oliveria, *Phys. Rev. Lett*., 1984, **52**, 1433–1437.
17 R. L. Whetten, J. T. Khoury, M. M. Alvarez, S. Murthy, I. Vezmar, Z. L. Wang, P. W. Stephens, C. L. Cleveland, W. D. Luedtke and U. Landman, *Adv. Mater*., 1996, **8**, 428–433.
18 S. L. Stoeva, B. L. V. Prasad, S. Uma, S. P. K. Stoimenov, V. Zaikovsky, C. M. Sorensen and K. J. Klabunde, *J. Phys. Chem. B*, 2003, **107**, 7441–7448.
19 D. V. Talapin, E. V. Shevchenko, C. B. Murray, A. V. Titov and P. Kral, *Nano Lett*., 2007, **7**, 1213–1219.
20 B. Abecassis, F. Testard and O. Spalla, *Phys. Rev. Lett*., 2008, **100**, 115504-1–115504-4.
21 P. J. Thomas, G. U. Kulkarni and C. N. R. Rao, *J. Phys. Chem. B*, 2000, **104**, 8138–8144.
22 L. O. Brown and J. E. Hutchison, *J. Phys. Chem. B*, 2001, **105**, 8911–8916.
23 C. J. Kiely, J. Fink, M. Brust, D. Bethell and D.J. Schiffrin, *Nature*, 1998, **396**, 444–446.
24 J. Fink, C. J. Kiely, D. Bethell and D. J. Schiffrin, *Chem. Mater*., 1998, **10**, 922–926.
25 J. E. Martin, J. P. Wilcoxon, J. Odinek and P. Provencio, *J. Phys. Chem. B*, 2000, **104**, 9475–9486.
26 M. Brust, D. Bethell, D. J. Schiffrin and C. J. Kiely, *Adv. Mater*., 1995, **7**, 795–797.
27 I. Hussain, Z. Wang, A. I. Cooper and M. Brust, *Langmuir*, 2006, **22**, 2938–2941.
28 C. R. Mayer, S. Neveu and V. Cabuil, *Adv. Mater*., 2002, **14**, 595–597.
29 D. S. Sidhaye, S. Kashyap, M. Sastry, S. Hotha and B. L. V. Prasad, *Langmuir*, 2005, **21**, 7979–7984.
30 C. Guarise, L. Pasquato and P. Scrimin, *Langmuir*, 2005, **21**, 5537–5541.
31 J. M. Wessels, H.-G. Nothofer, W. E. Ford, F. von Wrochem, F. Scholz, T. Vossmeyer, A. Schroedter, H. Weller and A. Yasuda, *J. Am. Chem. Soc*., 2004, **126**, 3349–3356.
32 R. Shenhar and V. M. Rotello, *Acc. Chem. Res*., 2003, **36** 549–561.
33 N. L. Rosi and C. A. Mirkin, *Chem. Rev*., 2005, **105**, 1547–1562.
34 S. I. Stoeva, A. B. Smetana, C. M. Sorensen and K. J. Klabunde, *J. Colloid Interface Sci*., 2007, **309**, 94–98.
35 S. Wang, S. Sato and K. Kimura, *Chem. Mater*., 2003, **15**, 2445–2448.
36 H. Yao, T. Minami, A. Hori, M. Koma and K. Kimura, *J. Phys. Chem. B*, 2006, **110**, 14040–14045.
37 (*a*) J. H. Fendler and F. C. Meldrum, *Adv. Mater*., 1994, **7**, 607–632; (*b*) J. H. Fendler, *Nanoparticles and Nanostructured Films: Preparation, Characterization and Applications*, Wiley-VCH, Weinheim, Germany, 1998.
38 B. Kim, S. L. Tripp and A. Wei, *J. Am. Chem. Soc*., 2001, **123**, 7955–7956.
39 H. Yao, H. Kojima, S. Sato and K. Kimura, *Langmuir*, 2004, **20**, 10317–10323.
40 Owing to space considerations it is difficult to include all the references of this group's work. Please see the references cited in (*a*) R. Pasricha, A. Swami and M. Sastry, *J. Phys. Chem. B*, 2005, **109**, 19620–19626; for reviews of their work in this field refer to; (*b*) M. Sastry, M. Rao and K. N. Ganesh, *Acc. Chem. Res*., 2002, **35**, 847–855; (*c*) M. Sastry, in *Colloids and Colloid Assemblies*, ed. F. Caruso, Wiley-VCH, Verlag GmbH, KgaA, Weinheim, p. 369.
41 A. Kumar, S. Mandal, S. P. Mathew, P. R. Selvakannan, A. B. Mandale, R. V. Chaudhari and M. Sastry, *Langmuir*, 2002, **18**, 6478–6483.
42 P. R. Selvakannan, S. Mandal, R. Pasricha, S. D. Adyanthaya and M. Sastry, *Chem. Commun*., 2002, 1334–1335.
43 C. N. R. Rao and K. P. Kalyanikutty, *Acc. Chem. Res*., 2008, **41**, 489–499.
44 V. V. Agrawal, G. U. Kulkarni and C. N. R. Rao, *J. Phys. Chem. B*, 2005, **109**, 7300–7305.
45 (*a*) P. C. Ohara and W. M. Gelbart, *Langmuir*, 1998, **14**, 3418–3424; (*b*) P. C. Ohara, J. R. Heath and W. M. Gelbart, *Angew. Chem., Int. Ed. Engl*., 1997, **36**, 1077–1080.
46 X. M. Lin, H. M. Jaeger, C. M. Sorensen and K. J. Klabunde, *J. Phys. Chem. B*, 2001, **105**, 3353–3357.
47 B. A. Korgel and D. Fitzmaurice, *Phys. Rev. Lett*., 1998, **80**, 3531–3534.
48 M. Aslam, I. S. Mulla and K. Vijayamohanan, *Langmuir*, 2001, **17**, 7487–7493.

49 (*a*) T. Vossmeyer, E. DeIonno and J. R. Heath, *Angew. Chem., Int. Ed. Engl.*, 1997, **36**, 1080–1083; (*b*) S. Liu, R. Maoz, G. Schmid and J. Sagiv, *Nano Lett.*, 2002, **2**, 1055–1060; (*c*) P. M. Mendes, S. Jacke, K. Critchley, J. Plaza, Y. Chen, K. Nikitin, R. E. Palmer, J. A. Preece, S. D. Evans and D. Fitzmaurice, *Langmuir*, 2004, **20**, 3766–3768.
50 (*a*) J. Sharma, R. Chhabra, Y. Liu, Y. Ke and H. Yan, *Angew. Chem., Int. Ed.*, 2006, **45**, 730–735; (*b*) A. Kumar, M. Pattarkine, M. Bhadbhade, A. B. Mandale, K. N. Ganesh, S. S. Datar, C. V. Dharmadhikari and M. Sastry, *Adv. Mater.*, 2001, **13**, 341–344.
51 S.-W. Chung, D. S. Ginger, M. W. Morales, Z. Zhang, V. Chandrasekhar, M. A. Ratner and C. A. Mirkin, *Small*, 2005, **1**, 64–69.
52 O. Vidoni, T. Reuter, V. Torma, W. Meyer-Zaika and G. Schmid, *J. Mater. Chem.*, 2001, **11**, 3188–3190.
53 J. Huang, A. R. Tao, S. Connor, R. He and P. Yang, *Nano Lett.*, 2006, **6**, 524–529.
54 M. Kanehara, E. Kodzuka and T. Teranishi, *J. Am. Chem. Soc.*, 2006, **128**, 13084–13094.
55 M. Kanehara, Y. Oumi, T. Sano and T. Teranishi, *J. Am. Chem. Soc.*, 2003, **125**, 8708–8709.
56 D. S. Sidhaye and B. L. V. Prasad, *Chem. Phys. Lett.*, 2008, **454**, 345–349.
57 (*a*) L. Wang, X. Shi, N. N. Kariuki, M. Schadt, G. R. Wang, Q. Rendeng, J. Choi, J. Luo, S. Lu and C.-J. Zhong, *J. Am. Chem. Soc.*, 2007, **129**, 2161–2170; (*b*) C. Guarise, L. Pasquato, V. De Filippis and P. Scrimin, *Proc. Natl. Acad. Sci. U. S. A.*, 2006, **103**, 3978–3982.
58 D. Roy and J. R. Fendler, *Adv. Mater.*, 2004, **16**, 479–508.
59 D. R. Smith, J. B. Pendry and M. C. K. Wiltshire, *Science*, 2004, **305**, 788–792.